Hopping Kinetics on a Finite 1D Chain: An Exact Analysis

J.-S. McEWEN,[1] S. H. PAYNE,[2] H. J. KREUZER,[2] C. BRACHER[3]

[1]*Center for Nonlinear Phenomena and Complex Systems, Campus Plaine CP 231, Université Libre de Bruxelles, B-1050 Brussels, Belgium*

[2]*Department of Physics and Atmospheric Science, Dalhousie University, Halifax, Nova Scotia B3H 3J5, Canada*

[3]*Physics Department, Bryn Mawr College, 101 N. Merion Ave., Bryn Mawr, Pennsylvania 19010, USA*

Received 7 March 2006; accepted 20 April 2006
Published online 24 July 2006 in Wiley InterScience (www.interscience.wiley.com).
DOI 10.1002/qua.21143

ABSTRACT: In the present study, we develop a kinetic lattice gas model for hopping in an inhomogeneous one-dimensional adsorbate system with nearest-neighbor interactions and periodic boundary conditions. From the matrices of the associated equations of motion, we can calculate adsorbate correlation functions in momentum space exactly on all time and length scales. The corresponding eigenvalues and eigenvectors in the long-time, long-wavelength limit yield the diffusion coefficient. We analyze its dependence on coverage and temperature and compare our results with earlier analytic work for this model. Our approach is readily extendable to two-dimensional systems. © 2006 Wiley Periodicals, Inc. Int J Quantum Chem 106: 2889–2903, 2006

Key words: lattice gas; nonequilibrium thermodynamics and statistical mechanics; models of surface kinetics; surface diffusion

1. Introduction

Various theoretical approaches have been applied to the study of diffusion in low-dimensional systems, from analytic methods based on the master, Fokker–Planck, or Kramers equations, to numerical methods based on Monte Carlo and molecular dynamics (MD) simulations. The former provide physical insight, although usually at the cost of some simplifying assumptions, and closed-form solutions in special cases. Simulation methods have the advantage of producing realistic, but numerical, results for particular physical systems. Several reviews exist and together cover all these approaches [1–4]. Required for all methods is a representation of the dynamics of the diffusing particle. For particles moving between well-defined lattice sites, the energy barrier can be calculated accurately by ab initio methods. However, this alone does not determine the dynamics [1], and approximations to the latter must be made, short of full-blown quantum mechanical treatments.

Correspondence to: J.-S. McEwen; e-mail: jmcewen@ulb.ac.be

Contract grant sponsors: NSERC; Office of Naval Research; Killam Trust; Alexander von Humboldt Foundation.

Diffusion, both tracer and collective, on the basis of the lattice gas model, has been studied since the pioneering work of Elliott [4, 5]. For this description, the usual starting point is the master equation with the hopping between lattice sites treated as a Markovian process; i.e., the residence time at sites is long compared with the time of individual hops. This is also the easiest route to incorporate the effects of multiple binding sites within cells and particle interactions, both hardcore within cells and short range between them. In the case of surface diffusion, such interactions lead to a strong dependence of the diffusivity on the coverage of the adspecies. The "dynamics" in this kinetic lattice gas model are usually simplified to the specification of transition probabilities with a hopping rate, usually of an Arrhenius form, but modified by interactions with neighboring particles. Again, there is a marked dependence of the diffusion for different choices of this modifier [3].

Except in some special cases, e.g., hardcore exclusion alone, analytic solutions for the diffusivity do not exist, and calculations must be made using linear response theory or Monte Carlo simulations. One case that admits an exact solution is the one-dimensional (1D) model of Zwerger [6], who expressed the collective diffusion coefficient, for certain choices of the dynamics on an infinite 1D lattice with nearest-neighbor interactions, in terms of equilibrium correlators. What is missing, even in this 1D case, is an exact solution of the time evolution of the system, prepared in a nonequilibrium configuration, and its subsequent passage to the long-time, large-length scale limit where macroscopic diffusion equations apply.

Regarding the latter, we note that Fick's equation for the particle current

$$\mathbf{J} = -D\nabla n(\mathbf{r}, t), \tag{1}$$

where $n(\mathbf{r}, t)$ is the number density only gives the standard diffusion equation when D is a constant. Otherwise, one has

$$\frac{\partial n(\mathbf{r}, t)}{\partial t} = \nabla D(n) \cdot \nabla n + D\nabla^2 n. \tag{2}$$

However, even the applicability of this equation can been questioned. For example, van Kampen has proposed the form [7]

$$\frac{\partial n}{\partial t} = \nabla^2 (D(n)n) \tag{3}$$

and has argued [8] that one cannot make any a priori choice of the form of the diffusion equation without examining the underlying mechanisms for a particular system.

In this work, we will set up the formalism that produces the evolution of a system on all time and length scales, relative to those of the characteristic time and length scales for local equilibrium [9] (here, the hopping time of an isolated particle and the lattice constant, respectively), and which permits examination of choices of the hopping mechanism. This is done by changing the representation of, and then solving the master equation for, the configuration probabilities of an adsorbate system with nearest-neighbor interactions on a finite 1D lattice.

This article is organized as follows. In Section 2, we introduce the kinetic lattice gas model and the assumptions for the site transition rates. In Section 3, we develop the formalism, for a 1D chain, that transforms the solution of the master equation into the problem of determining the eigenvalue spectrum of the transition rate matrix; this allows the time evolution of any particle correlator to be constructed explicitly. In Section 4, we present results of calculations and interpretations of this spectrum for lattices of varying size, we obtain the diffusion coefficient and compare them with the results of Zwerger, and we exhibit the complete time evolution of average site occupations for some initial conditions. Section 5 concludes with a summary and an outlook to applications to 1D and 2D systems.

2. Kinetic Lattice Gas Model

To set up the kinetic lattice gas model, one assumes that the surface of a solid can be divided into N_s sites (or cells) labeled l, for which one introduces microscopic occupation numbers n_l as 1 or 0, depending on whether or not site l is occupied by an adsorbed particle. There are 2^{N_s} microstates $\mathbf{n} = (n_1, n_2, \ldots, n_{N_s})$ given by sequences of 0 and 1. To introduce the dynamics of the system, one writes down a model Hamiltonian, here in one dimension with periodic boundary conditions:

$$H(\mathbf{n}) = E_s \sum_{l=1}^{N_s} n_l + V_1 \sum_{l=1}^{N_s} n_l n_{l+1}. \tag{4}$$

Arguing that the lattice gas Hamiltonian should give the same Helmholtz free energy as a microscopic Hamiltonian (for noninteracting particles), it

can be shown that the proper identification of E_s in the canonical ensemble is the free energy per particle [10,11]:

$$E_s = -V_0 - k_B T \ln(q_3 q_{\text{int}}), \tag{5}$$

with V_0 the depth of the surface potential. The center-of-mass vibrations of the adsorbed molecule in this potential well are represented by the partition functions $q_3 = q_z q_{xy}$, with normal (z) and in-plane (x,y) components; $q_{\text{int}} = q_{\text{vib}} q_{\text{rot}}$ is the partition function for the internal degrees of freedom. These modes are usually described by 1D harmonic oscillators. V_1 is the two-particle interaction between nearest neighbors. Extension to longer-range interactions and many-body interactions can also be included in Eq. (4).

We introduce a function $P(\mathbf{n}, t)$, which gives the probability that a given microstate $\mathbf{n}$ is realized at time t and define the transition probability per unit time, $W(\mathbf{n}', \mathbf{n})$, for the state $\mathbf{n}$ to change to $\mathbf{n}'$. The net change of the probability is incorporated in the master equation

$$\frac{dP(\mathbf{n}, t)}{dt} = \sum_{\mathbf{n}'} \left[W(\mathbf{n}, \mathbf{n}') P(\mathbf{n}', t) - W(\mathbf{n}', \mathbf{n}) P(\mathbf{n}, t) \right]. \tag{6}$$

For long enough times the system will reach a steady state. We guarantee that this state will be the equilibrium one, independent of time, $P(\mathbf{n}', t \to \infty) \to P_{\text{eq}}(\mathbf{n})$, by imposing the condition of detailed balance, which requires that each term on the right-hand side of Eq. (6) vanish:

$$W(\mathbf{n}, \mathbf{n}') P_{\text{eq}}(\mathbf{n}') = W(\mathbf{n}', \mathbf{n}) P_{\text{eq}}(\mathbf{n}). \tag{7}$$

If the number of particles in the adsorbate is fixed, this equilibrium distribution is given by

$$P_{\text{eq}}(\mathbf{n}) = Z^{-1} \exp(-H(\mathbf{n})/k_B T), \tag{8}$$

where Z is the canonical partition function. Provided the residence time of an adparticle at a site is long compared with the transit times into and out of the site, we can write $W(\mathbf{n}', \mathbf{n})$ as a sum of terms representing the separate processes of adsorption, desorption, and hopping. In principle, $W(\mathbf{n}', \mathbf{n})$ must be calculated from a Hamiltonian that includes, in addition to Eq. (4), coupling terms to the gas phase and the substrate that mediate mass and energy exchange. In this paper we will rather follow the procedure initiated by Glauber [12] in setting up the kinetic Ising model and specify appropriate forms of $W(\mathbf{n}', \mathbf{n})$. We shall also only be concerned with the diffusion of a fixed number of adparticles; the development of the model to describe adsorption–desorption kinetics is fully discussed elsewhere [13].

The most general form that one can write for the transition probability to treat the hopping of a particle between neighboring sites [13] is

$$\begin{aligned} W_{\text{diff}}(\mathbf{n}', \mathbf{n}) = J_0 \sum_{i,a} n_i (1 - n_{i+a}) \Bigg[1 + A_1 \sum_{a' \neq a} n_{i+a'} \\ + B_1 \sum_{a' \neq -a} n_{i+a+a'} + C_1 \sum_{a' \neq a} n_{i+a'} \sum_{a' \neq -a} n_{i+a+a'} \Bigg] \\ \times \delta(n_i', 1 - n_i) \delta(n_{i+a}', 1 - n_{i+a}) \prod_{l \neq i, i+a} \delta(n_l, n_l'). \end{aligned} \tag{9}$$

Here, for example, hopping of a particle at site i to site $i+a$ occurs if $n_i = 1, n_{i+a} = 0$ initially, with a rate controlled by existing or prospective neighbors if the coefficients A_1, B_1, or C_1 are nonzero. The Kronecker delta for sites $l \neq i, i+a$ excludes multiple transitions. Application of the detailed balance condition imposes only one constraint on the coefficients:

$$1 + B_1 = (1 + A_1) e^{-\beta V_1}. \tag{10}$$

For a 1D lattice, Eq. (9) can be rewritten to represent the four distinct hopping environments explicitly:

$$\begin{aligned} W_{\text{diff}}(\mathbf{n}', \mathbf{n}) = J_0 \sum_i \{ n_i (1 - n_{i+1}) [(1 - n_{i-1})(1 - n_{i+2}) \\ + (1 + A_1) n_{i-1} (1 - n_{i+2}) + (1 + B_1)(1 - n_{i-1}) n_{i+2} \\ + (1 + A_1 + B_1 + C_1) n_{i-1} n_{i+2}] + (1 - n_i) n_{i+1} \\ \times [(1 - n_{i-1})(1 - n_{i+2}) + (1 + A_1)(1 - n_{i-1}) n_{i+2} \\ + (1 + B_1) n_{i-1} (1 - n_{i+2}) + (1 + A_1 + B_1 + C_1) n_{i-1} n_{i+2}] \} \\ \times \delta(n_i, 1 - n_i') \delta(n_{i+1}, 1 - n_{i+1}') \prod_{l \neq i, i+1} \delta(n_l, n_l'). \end{aligned} \tag{11}$$

The first term in each square bracket represents the hopping of an isolated particle with a rate J_0 (α_2 in the notation of [3]); the second term represents the separation of a particle from (a neighboring block of) particles with a rate $\alpha_3 = J_0(1 + A_1)$, with no neighbors after the hop; the converse of this is the third term, rate $\alpha_4 = J_0(1 + B_1)$; the last term exhibits the exchange of a particle between blocks with a rate $\alpha_1 = J_0(1 + A_1 + B_1 + C_1)$. The four processes are illustrated in Figure 1.

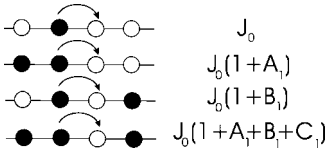

FIGURE 1. The four possible hopping processes in a one-dimensional adsorbate system that occur with various rate factors.

Because detailed balance does not fix all the coefficients in the transition probability, any functional relation between the coefficients must be postulated, based on physical arguments, or calculated from a microscopic Hamiltonian that accounts for the coupling of the adsorbate to the lattice or electronic degrees of freedom of the substrate [14]. Not surprisingly, such relations are not unique; they reflect the fact that different systems can have different kinetics. Various choices have been made in the literature [3, 13]. Here we shall treat the initial and final state for a hopping event on an equal footing. This is accomplished with interaction kinetics [13, 15]:

$$A_1 = -B_1. \tag{12}$$

Moreover, to preserve particle hole symmetry, we will require that

$$\alpha_1 + \alpha_2 - \alpha_3 - \alpha_4 = J_0 C_1 = 0. \tag{13}$$

This condition was originally considered by Singer and Peschel [16] in the context of lattice models of ionic conductivity and by Zwerger [6] in his closed-form solution for the diffusion coefficient.

Experimental variables or quantities related to them are obtained by averaging single-site or multisite occupations over all microscopic configurations of the adsorbate. Thus the average occupation at a particular site (the local coverage) is defined by

$$\langle n_l \rangle(t) = \sum_{\mathbf{n}} n_l P(\mathbf{n}, t) \tag{14}$$

and the total adsorbate coverage as

$$\theta(t) = \frac{1}{N_s} \sum_{l=1}^{N_s} \langle n_l \rangle(t). \tag{15}$$

The time evolution of such average quantities follows from Eq. (6) directly; there is an equation of motion for each correlator. Because these equations are coupled, e.g., that for $\langle n_l \rangle(t)$ contains two-, three-, and four-site nearest-neighbor correlators (see Appendix A), an infinite hierarchy of equations is generated. For a solution, this hierarchy must be truncated. One method, which has been successfully applied to 1D homogeneous systems, is to factor higher-order correlators in terms of lower-order ones. Complications arise with this approach in two dimensions: the nonlinearities introduced in one dimension usually become unstable in two [17]. Here, instead, we will truncate the equations such that they remain linear in one dimension, or two, by assuming a finite lattice.

3. Finite Lattice Approach

3.1. DEFINITIONS

We consider a finite 1D lattice with periodic boundary conditions, i.e., a ring of N_s sites, on which the adsorbate can diffuse by jump events in which a single particle leaves its site and occupies a neighboring empty site. The ring has length $L = N_s a$, where a is the lattice constant. We index the sites, clockwise from a reference site, as $l = 0, 1, \ldots, N_s - 1$. We term two arrangements (states) of N particles on these N_s sites as equivalent if a simple rotation of the entire occupation pattern of one transforms it into the other. For such states it suffices to select one member of each set of equivalent states (the equivalence class) as a representative; we call this state the primitive. To distinguish the members of the class, we define a pattern sum, σ by

$$\sigma = \sum_{l=0}^{N_s-1} l\delta(n_l, 1) \ (\mathrm{mod} N_s), \tag{16}$$

as the sum over the occupation numbers of the pattern on the ring. If we choose N_s to be prime and employ modulo arithmetic, we find that (i) there are exactly N_s equivalent states, each of which can be obtained by a (clockwise) rotation, or shift, by $s = 0, 1, \ldots, N_s - 1$ sites of the primitive pattern; and (ii) the pattern sums of these states are distinct and assume the (generally noncorresponding) values $\sigma = 0, 1, \ldots, N_s - 1$. We designate the arrangement with $\sigma = 0$ as the primitive. In particular, a rotation of any pattern by m sites will change its pattern sum by an amount $\sigma' - \sigma = mN(\mathrm{mod} N_s)$. Thus, instead of listing the occupation numbers $(n_1, n_2, \ldots, n_{N_s})_N$, we can specify a configuration of particles uniquely with the index of the primitive

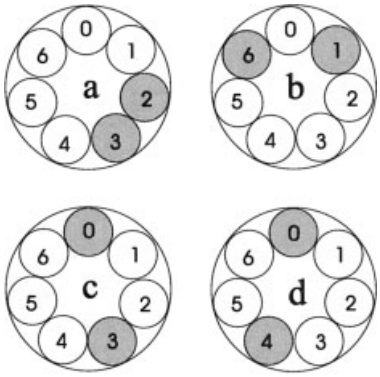

FIGURE 2. Four of 21 possible arrangements, of two particles on a 7-site ring ($N_p = 3$) with state indices, $[p|s]$, and pattern sums, σ, (a) $[p_1|6], 5$; (b) $[p_2|0], 0$; (c) $[p_3|5], 3$; and (d) $[p_3|2], 4$. State (b) is one of the three primitives.

pattern, p, of its equivalence class and its shift number, s, relative to this primitive; we label this state as $[p|s]$. As for the primitives, there are $\binom{N_s}{N}$ arrangements of N particles on N_s sites, so the number of primitive patterns is

$$N_p = \frac{1}{N_s}\binom{N_s}{N}. \tag{17}$$

We denote this set of primitives, for N fixed, by $\mathbf{p} = (p_1, p_2, \ldots, p_{N_p})$. An example of the indexing of some configurations is given in Figure 2. Note that if a pattern is reflected in the plane passing through the reference site, its pattern sum reverses sign, $\sigma \to -\sigma$. However, the primitive of the image pattern may differ. Primitives necessarily transform into other primitives, generally, under this operation.

3.2. REPRESENTATIONS OF THE MASTER EQUATION

The probability of any given state $[p|s]$ evolves in time due to jumps of particles into neighboring sites. Generally, a single-site jump will change both the primitive and the shift number, $[p|s] \to [p'|s']$, but the pattern sum can only change by unity, $\sigma \to \sigma' = \sigma \pm 1$, where the positive (negative) sign corresponds to clockwise (counterclockwise) jumps. The relation $\sigma = sN(\mathrm{mod}N_s)$ then constrains the change of the shift number (rotation of the pattern), $\Delta s = s' - s$,

$$\Delta sN = \pm 1(\mathrm{mod}N_s). \tag{18}$$

So, regardless of the primitives associated with the transition, Δs is fixed by N. This allows the master equation to be recast: The transition rates between microstates can only depend on the primitive index; we denote (counter) clockwise jump rates, from primitive p to primitive p', by

$$W_{\circlearrowleft}(p', p), W_{\circlearrowright}(p', p). \tag{19}$$

The master equation (6) has two parts, the loss of probability of a given configuration due to jumps into other configurations and the gain through the reverse jumps from the latter. If the first part is represented by the net jump rate,

$$W_{\bigcirc}(p) = \sum_{p' \in \mathbf{p}} \left[W_{\circlearrowleft}(p', p) + W_{\circlearrowright}(p', p) \right], \tag{20}$$

then the time evolution of the probability of the microstate $[p|s]$, $P(p, s, t)$, is seen to be governed by the equation:

$$\begin{aligned} \frac{dP(p,s,t)}{dt} &= -W_{\bigcirc}(p)P(p,s,t) \\ &\quad + \sum_{p' \in \mathbf{p}} W_{\circlearrowleft}(p, p')P(p', s - \Delta s, t) \\ &\quad + \sum_{p' \in \mathbf{p}} W_{\circlearrowright}(p, p')P(p', s + \Delta s, t). \end{aligned} \tag{21}$$

This represents one member of the $N_p \times N_s$ equations, which describe the evolution of the N particles on the ring; the complete solution is a vector of microstate probabilities $\mathbf{P}(t) = \{P(p_i, s, t), i = 1 \ldots N_p, s = 0 \ldots N_s - 1\}$. With this solution, configuration-averaged site occupations and multi-site correlators at any given time may be obtained in the occupation number representation by summation over all matching patterns in $\mathbf{P}$. For example,

$$\langle n_l \rangle(t) = \sum_{s=0}^{N_s - 1} \sum_{p \in \mathbf{p}} P(p, s, t)\Theta([p|s], n_l), \tag{22}$$

where $\Theta([p|s], n_l) = 1, 0$ as the lth site in the pattern $[p|s]$ is occupied or not.

3.3. RECIPROCAL SPACE REPRESENTATION

The transition matrix operating in Eq. (21) couples states differing by Δs. However, the relative separations of adparticles for members of an equivalence class are independent of s. We exploit this rotational invariance and decouple the system of equations by transforming to reciprocal space.

We define a discrete Fourier transform of $P(p,s,t)$,

$$\widetilde{P}(p,q,t) = \frac{1}{N_s}\sum_{s=0}^{N_s-1} e^{-2\pi iqs/N_s} P(p,s,t), \qquad (23)$$

with $q = 0, 1, \ldots, N_s - 1$ indexing the reciprocal lattice vector. Note that because it is complex, $\widetilde{P}(p,q,t)$ cannot be interpreted as a probability. Performing the transform of both sides of Eq. (21), we obtain a set of N_s equations, one for each value of q:

$$\frac{d\widetilde{P}(p,q,t)}{dt} = \sum_{p'\in\mathbf{p}} W(p,p';q)\widetilde{P}(p',q,t), \qquad (24)$$

where

$$W(p,p';q) = -W_{\circlearrowright}(p)\delta_{p,p'} + e^{-2\pi iq\Delta s/N_s} W_{\circlearrowright}(p,p') + e^{2\pi iq\Delta s/N_s} W_{\circlearrowleft}(p,p'). \qquad (25)$$

These equations define the evolution of one component of a vector $\widetilde{\mathbf{P}}(q,t) = \{\widetilde{P}(p_i,q,t), i = 1 \ldots N_p\}$ and the elements of a matrix, $\mathbf{W}(q)$, of dimensions $N_p \times N_p$, respectively. The complete evolution is

$$\frac{d\widetilde{\mathbf{P}}(q,t)}{dt} = \mathbf{W}(q)\cdot\widetilde{\mathbf{P}}(q,t), \qquad (26)$$

with the formal solution

$$\widetilde{\mathbf{P}}(q,t) = \exp(t\mathbf{W})\cdot\widetilde{\mathbf{P}}(q,0). \qquad (27)$$

This can be reexpressed straightforwardly if $\mathbf{W}(q)$ is first transformed to a diagonal matrix. As the transition rates represented by $W_{\circlearrowright}$ and $W_{\circlearrowleft}$ are real, we have that

$$W(p,p';q)^* = W(p,p';N_s - q); \qquad (28)$$

i.e., the matrices with reciprocal lattice vectors q and $-q(\mathrm{mod}\, N_s)$ are complex conjugates of each other. A corresponding relation exists for $\widetilde{P}(p,q,t)$. Thus, only the values $q = 0, 1, \ldots, (N_s-1)/2$ need be considered in the solution procedure.

The diagonalization of $\mathbf{W}(q)$ defines eigenvalues, $-\lambda_\alpha(q)$, and associated right eigenvectors, $\mathbf{u}_\alpha(q)$, $\alpha = 1, \ldots, N_p$,

$$\mathbf{W}\cdot\mathbf{u}_\alpha = -\lambda_\alpha\mathbf{u}_\alpha. \qquad (29)$$

Because $\mathbf{W}$ is not symmetric there are associated left eigenvectors, $\mathbf{v}_\alpha(q)$, which satisfy $\mathbf{v}_\alpha\cdot\mathbf{u}_\beta = \delta_{\alpha\beta}$. In terms of these quantities the solution (27) becomes

$$\widetilde{\mathbf{P}}(q,t) = \sum_{\alpha=1}^{N_p} \mathbf{u}_\alpha A_\alpha(q)\exp(-\lambda_\alpha t), \qquad (30)$$

with the initial conditions entering via the expansion coefficients,

$$A_\alpha(q) = \mathbf{v}_\alpha\cdot\widetilde{\mathbf{P}}(q,t=0). \qquad (31)$$

3.4. SPECIAL EIGENVECTORS: SYMMETRIZATION OF THE MATRIX

We note that the matrix $\mathbf{W}(q=0)$ is both real and singular; the latter condition follows by summing $W(p,p';0)$ over p and using Eqs. (25) and (20). The one vanishing eigenvalue for $q = 0$, and hence the vanishing temporal evolution, corresponds to the equilibrium configuration of the adsorbate. The corresponding eigenvectors are related to the equilibrium distribution [14]. In particular, to within a normalization factor, the pair of the associated eigenvectors is given by $\mathbf{v}_{\alpha=1}(q=0) = (1,1,\ldots,1)^T$, the unit vector, and $\mathbf{u}_{\alpha=1}(q=0) = \mathbf{P}_{\mathrm{eq}}$, where

$$P_{\mathrm{eq}}(p) = Z^{-1}\exp(-H(p)/k_BT) \qquad (32)$$

is the canonical probability distribution for the primitives. This distribution can be used to symmetrize $\mathbf{W}(q)$. The transition rates (19) must satisfy detailed balance:

$$W_{\circlearrowright}(p,p')P_{\mathrm{eq}}(p') = W_{\circlearrowleft}(p',p)P_{\mathrm{eq}}(p). \qquad (33)$$

Together with the diagonal matrix,

$$S(p',p) = \sqrt{\frac{P_{\mathrm{eq}}(p)}{N_s}}\delta_{p,p'}, \qquad (34)$$

we use Eq. (33) to construct a symmetric Hermitian matrix, $\mathbf{W}_s$, with the similarity transformation

$$\mathbf{W}_s(q) = \mathbf{S}^{-1}\mathbf{W}(q)\mathbf{S}. \qquad (35)$$

Thus, the eigenvalues of $\mathbf{W}$ are all real and, indeed, are all non-negative (i.e., $\lambda_\alpha(q) \geq 0$) [14].*

*The factor of N_s in (34) arises from the normalization of the equilibrium eigenvectors, $N_s\sum_p P_{\mathrm{eq}}(p) = 1$.

3.5. EIGENVALUE WEIGHTS

Armed with the eigenvectors, $\mathbf{u}_\alpha^s$, of $\mathbf{W}_s$ we reverse the sequence of transformations above: pre(post) multiplication of $\mathbf{u}_\alpha^{(s)}(\mathbf{u}_\alpha^{(s)\dagger})$ by $\mathbf{S}(\mathbf{S}^{-1})$ produces $\mathbf{u}_\alpha(\mathbf{v}_\alpha)$ and hence the solution vector (30); the inverse Fourier transform to Eq. (23) is applied to express both this vector and, separately, its initial value in terms of the real-space probability vectors, $\mathbf{P}(t)$ and $\mathbf{P}(0)$; lastly, $\mathbf{P}(t)$ is transformed to the occupation number representation, as in Eq. (22). For simplicity, and with little loss of generality, we choose a pure state $[p_o|s_o]$ as the initial state, $P(p,s,t=0) = \delta(p,p_o)\delta(s,s_o)$. Then, after some manipulations, we find that

$$\langle n_l\rangle(t) = \sum_{\alpha=1}^{N_p}\sum_{q=0}^{N_s-1} e^{2\pi iq(l-s_o)/N_s} v_\alpha(p_o,q)C_\alpha(q) \times \exp(-\lambda_\alpha(q)t), \quad (36)$$

with the coefficients

$$C_\alpha(q) = \widetilde{\mathbf{\Theta}}(q)\cdot\mathbf{u}_\alpha(q) \quad (37)$$

being weights associated with each eigenvalue, indexed by α and wavenumber q. The component of the vector, $\widetilde{\mathbf{\Theta}}(q)$, indexed by the primitive p is just the discrete Fourier transform of the pattern-matching function for that primitive

$$\widetilde{\Theta}(p,q) = \frac{1}{N_s}\sum_{m=0}^{N_s-1} e^{-2\pi iqm/N_s}\Theta([p|0],n_m) \quad (38)$$

and is independent of the interactions between the particles. The summand of Eq. (36) is the product of factors associated with the initial configuration, time-independent weights (37) and an exponential function of time. This equation represents the complete time evolution of the average occupation of an indexed site. The eigenvalue weights are central to our evaluation of the diffusivity of the lattice gas. Generally, among eigenvalues of similar magnitude, the contribution to the time evolution of $\langle n_l\rangle$ is due only to those that have significant values of $|C_\alpha(q)|$. We show in Appendix B that the weights can be chosen real and, if we have particle-hole symmetry in addition, that $C_\alpha(q\neq 0)$ changes sign around $\theta = 1/2$ ML.

3.6. CALCULATION PROCEDURE

Having established the necessary equations of our approach, we comment briefly on the algorithm for the solution of the time evolution of an arbitrary number of particles. We establish an ordered list of primitive patterns, using standard bit shifting techniques; the latter can also be used to calculate the corresponding equilibrium probabilities, (32), which form the equilibrium eigenvector $\mathbf{u}_{\alpha=1}^{(s)}(0)$. We examine all possible clockwise and counterclockwise jumps for all primitive patterns to construct $W_{\circlearrowleft}(p',p)$,$W_{\circlearrowright}(p',p)$ and $W_{\bigcirc}(p)$, as defined in Eqs. (19) and (20), and thus $\mathbf{W}(q)$. We symmetrize this matrix as in (35) and then use standard numerical techniques (Householder tri-diagonalization, QR algorithm [18]) to establish its eigenvalues, λ_α, and the eigenvectors, $\mathbf{u}_\alpha^s(q)$. The eigenvalue weights, Eq. (37), are then evaluated.

To obtain the time evolution of any desired configurational average, not just single-site distributions, we create a lookup table that contains matching information for each average to be calculated and translate the initial configuration of a given state $P(p,s,t=0)$ into reciprocal space to form $(N_s+1)/2$ initial vectors, $\widetilde{\mathbf{P}}(q,t=0)$. We multiply these vectors by the symmetrizing matrix $\mathbf{S}^{-1}$, and subsequently with the transformation matrix $\mathbf{U}^s(q)^\dagger$ formed by the eigenvectors $\mathbf{u}_\alpha^s(q)$. For each time step t, we multiply the resulting vectors with the appropriate time dependence, $\exp(-\lambda_\alpha t)$, and complete the similarity transformation by multiplying these vectors with $\mathbf{SU}^s(q)$, to obtain $\widetilde{\mathbf{P}}(q,t)$. We then perform the inverse of the transform (23) to obtain $\mathbf{P}(t)$ and use expressions such as (22) to obtain the required averages.

4. Results

4.1. DIFFUSION COEFFICIENT

We first consider the time evolution and the diffusion of a noninteracting 1D adsorbate, with only site exclusion operating, as a basis for comparison with the interacting case. The coverage, $\theta = N/N_s$, is arbitrary. The first equation of motion (cf. Appendix A) reduces to

$$\frac{d}{dt}\langle n_l\rangle(t) = J_0[\langle n_{l-1}\rangle(t) - 2\langle n_l\rangle(t) + \langle n_{l+1}\rangle(t)]. \quad (39)$$

With periodic boundary conditions, this is easily solved by transforming to reciprocal space

$$\tilde{n}_q(t) = \frac{1}{N_s}\sum_{l=0}^{N_s-1} e^{-2\pi iql/N_s}\langle n_l\rangle(t) \quad (40)$$

for which we get

$$\frac{d\tilde{n}_q(t)}{dt} = J_0(e^{2\pi iq/N_s} + e^{-2\pi iq/N_s} - 2)\tilde{n}_q(t) = -\lambda(q)\tilde{n}_q(t), \quad (41)$$

where

$$\lambda(q) = 4J_0 \sin^2\left(\frac{\pi q}{N_s}\right) = 4\,J_0 \sin^2\left(\frac{ka}{2}\right), \quad (42)$$

with $k = 2\pi q/L$. The dependence of this eigenvalue on q is illustrated in Figure 3 (dashed line). Solving this initial value problem and transforming back, we get

$$\langle n_l\rangle(t) = \frac{1}{N_s}\sum_{m=0}^{N_s-1}\left\{\sum_{q=0}^{N_s-1} e^{2\pi iq(l-m)/N_s} e^{-\lambda(q)t}\right\}\langle n_m\rangle(0). \quad (43)$$

Alternatively, we could have used the approach developed in Section 3 to solve the problem. Then one has $N_p(N)$ eigenvalues for each value of q, of which one (indexed as α_1) is given by Eq. (42); the remaining $N_p - 1$ eigenvalues, for each q, do not contribute to the time evolution of $\langle n_l\rangle(t)$ because their corresponding weights, $C_\alpha(q), \alpha \neq \alpha_1$, vanish. However, these eigenvalues do contribute to the time evolution of higher-order correlators, such as two- and three-particle. One can show that the weights for the nonvanishing eigenvalues (42) are given by

$$C_\alpha(q) = \begin{cases} \theta, & q = 0 \\ \sqrt{\frac{\theta(1-\theta)}{N_s-1}}, & q \neq 0, \theta < 0.5\ \text{ML} \\ -\sqrt{\frac{\theta(1-\theta)}{N_s-1}}, & q \neq 0, \theta > 0.5\ \text{ML} \end{cases} \quad (44)$$

We now consider the diffusivity. This derives immediately from Eq. (39) in the continuum limit, $N_s \to \infty, a \to 0, L = N_s a$ constant. With the replacement $\langle n_l\rangle(t) \to n(x = la, t) = \theta(x, t)$, and subsequent Taylor expansions of the right-hand side of Eq. (39), we recover Eq. (2) (in 1D) with $D = J_o a^2 \equiv D_0$ [19]. We may also obtain this result by a less direct route. We start with the spatial Fourier transform of (2) in 1D. Neglecting the spatial gradient of D we have

$$\frac{d\tilde{n}(k,t)}{dt} + Dk^2\tilde{n} = 0, \quad (45)$$

and we generate the finite-lattice equivalent as $\tilde{n}(k = 2\pi q/L, t) \to \tilde{n}_q(t)$. Upon substitution of the solution (41), we get

$$\left[-\lambda(q) + D\left(\frac{2\pi q}{L}\right)^2\right]\tilde{n}_q(0)\exp(-\lambda(q)t) = 0. \quad (46)$$

The diffusivity is strictly defined only in the long-time, long-wavelength limit; i.e., the first factor is necessarily zero as $t \to \infty, q/L \to 0$, and we recover $D = D_0$.

Our calculation of the diffusivity when adatom interactions are present follows this latter route. In this case, the generalization of (46) is

$$\sum_{\alpha=1}^{N_p}\left[-\lambda_\alpha(q) + D\left(\frac{2\pi q}{L}\right)^2\right] e^{-2\pi iqs_o/N_s} v_\alpha(p_o, q) C_\alpha(q) \times \exp(-\lambda_\alpha(q)t) = 0. \quad (47)$$

For long times, only exponential factors in the summand with small (nonzero) eigenvalues survive. Strictly, we need only consider the smallest such eigenvalue, $\lambda_\sigma(q)$, for which we must have

$$D = \lim_{q\to 0}\left(\frac{L}{2\pi q}\right)^2 \lambda_\sigma(q), \quad (48)$$

provided $C_\sigma(q \to 0)$ is finite. Inspection of the eigenvalue spectrum for arbitrary interaction shows that $\lambda_\sigma(q)$ need not remain the smallest eigenvalue as q increases; there may exist many comparable eigenvalues. However, and importantly, their contribution to the summand of (47) can be discriminated by their weights. Our method, then, to obtain the diffusion coefficient is to examine, simultaneously, the eigenvalues resulting from the diagonalisation of the matrix of transition rates at a given value of q and their corresponding weights. We can conveniently represent both quantities in one plot, consisting of the values of $|C_\alpha(q)|$ shown as points on a surface with the corresponding eigenvalue and the wavenumber, q, acting as plane coordinates.

As an example, we show the eigenvalue spectrum resulting for a system of 2 and 7 particles on 19 sites ($\theta = 2/19, 7/19$) with strong nearest-neighbor repulsions, $\beta V_1 = 5$, and interaction kinetics (Fig. 3). The ordinate has been scaled to yield the ratio of diffusion coefficients, D/D_0, in the hydrodynamic limit. To represent the variation of the weights, we have introduced color-coded intervals, as shown in the legend

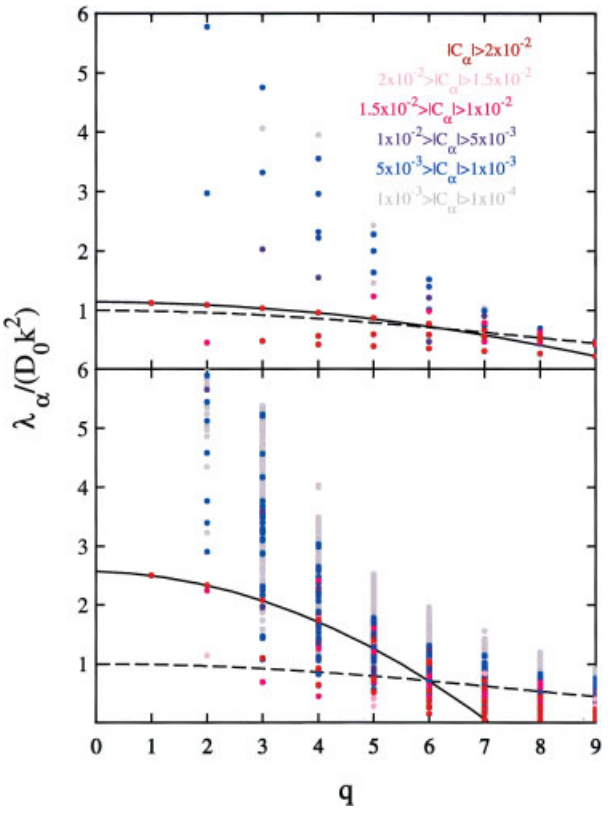

FIGURE 3. The eigenvalue spectrum as a function of wavenumber q, at coverages of 2/19 ML (upper panel) and 7/19 ML (lower panel) on a 19-site 1D lattice with nearest-neighbor repulsion ($\beta V_1 = 5$) and interaction kinetics. The color code for each eigenvalue indicates the magnitude of its weight, $|C_\alpha(q)|$, in the time evolution of the average site occupation. Solid line, a quadratic in q fitted through selected eigenvalues with $|C_\alpha(q)| > 0.02$ at $q = 1, 2, 3$; dashed line: dependence of the eigenvalues on q for a noninteracting adsorbate. The eigenvalue $\lambda = 0$ at $q = 0$ is not shown.

of Figure 3. It is immediately apparent that only *one* eigenvalue has significant weight at the smallest non-zero value of q. This feature is independent of lattice size, coverage, and interaction strength. Moreover, at $q = 0$, all the eigenvalue weights vanish except that for $\lambda = 0$, which gives the equilibrium solution. This delta function-like behavior of the eigenvalue weights at $q = 0$ can be understood by examining Eq. 40, from which we have $\tilde{n}_{q=0}(t) = \theta$, independent of time and interaction strength. The other eigenvalues could only contribute to $\tilde{n}_{q=0}(t)$ if adsorption and desorption events were allowed to occur. Obviously, there is no information about diffusion from this single vanishing eigenvalue.

To extract the diffusivity from such plots and in accord with its definition (48), we assume the expansion $\lambda/k^2 = D + \tilde{A}q + \tilde{B}q^2 + O(q^3)$. We obtain the coefficients by fitting the eigenvalues with the largest weights for $q = 1, 2, 3$, specifically, by including the maximally weighted eigenvalue at $q = 1$ and selecting among those with $|C_\alpha(q)| > C_m$ for $q > 1$. The cutoff value C_m is somewhat arbitrary; it was chosen to have enough eigenvalues to allow an estimate of the error in D by fitting at $q = 2, 3$ with eigenvalues of slightly differing weights; the cutoff also depends on V_1; e.g., for $\beta V_1 = 5$, a value of 0.02 was used, but for $\beta V_1 = -5$, a value of 0.2 was necessary. The results of the 3-point fits are shown as solid lines in

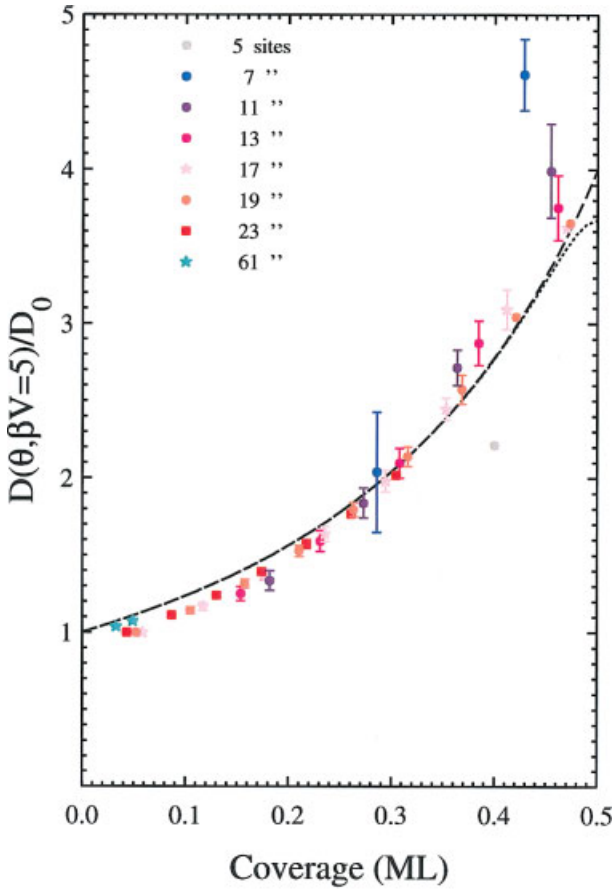

FIGURE 4. The diffusion coefficient as a function of coverage with nearest-neighbor repulsions ($\beta V_1 = 5$) and interaction kinetics for varying lattice size. (The method of obtaining the error bars is described in the text.) Lines: Zwerger's result [6] for an infinite lattice with $\beta V_1 = 5$ (dotted) and $\beta V_1 \to \infty$ (long-dashed). The few points beyond 0.25 ML without error bars were estimated uniquely from the eigenvalue spectrum at $q = 1$.

Figure 3; the value of D/D_0 is given by the intercept. Gratifyingly, the extrapolations of the fits to $q > 3$ agree very well with a significant number of other eigenvalues there with $|C_\alpha(q)| > 0.02$. We find that the coefficient $\tilde{A}$ is orders of magnitude smaller than D and decreases rapidly with increasing lattice size; e.g., it changes from 0.046 (upper panel) to 0.0028 (lower panel) and is as small as 0.00002 for $\theta = 3/61$. One expects this coefficient to vanish, since it corresponds to an even power of the density gradient in the particle current expression. The absolute value of $\tilde{B}$ is analogous to the super-Burnett coefficient [20], B^*, which occurs as the first correction to the tracer diffusion coefficient:

$$B^* = \lim_{t\to\infty} \frac{1}{4!t}\left[\langle (x(t)-x(0))^4\rangle - 3\langle (x(t)-x(0))^2\rangle^2\right]. \tag{49}$$

Although we are evaluating the collective diffusion coefficient in this work, it is of interest to note that our value of $B = \left(\frac{L}{2\pi}\right)^2\tilde{B}$ at 3/61 ML for $\beta V = 5$ is about -0.1 and becomes more negative as the coverage is increased. This is in rough agreement with the noninteracting case, for which the two diffusivities are identical and for which the Taylor expansion of (42) produces the term $-k^4/6$.

By repeating the fitting procedure at different coverages we can obtain the diffusion coefficient as a function of coverage. This is shown in Figure 4 and for various numbers of sites. Here we include estimates of the uncertainty of D. This estimate is largest around 1/2 ML and for systems with small numbers of adsorption sites (e.g., 7 sites); it is precisely for these conditions that the dominating eigenvalues with significant weights vary rapidly with q. As the number of sites increases and the coverage decreases the peaks associated with the surface of maximal eigenvalue-weights sharpen and the uncertainty in D decreases. Because we have imposed particle hole symmetry, D is symmetric around 1/2 ML. (Note that for infinite nearest-neighbor repulsion, the adsorbate coverage must saturate at 1/2 ML.) We remark that our approach and the accuracy of the analysis is not limited to large values of βV_1; we have only selected a strong repulsion because the diffusion coefficient shows the greatest variation as a function of coverage. As βV_1 decreases so does the diffusion coefficient, at fixed coverage, to D_0 at $\beta V_1 = 0$, where it becomes independent of coverage. For attractive interactions, D decreases with increasing coverage up to 1/2 ML and rises back to D_0 at 1 ML. It vanishes at 1/2 ML for infinite attraction.

To further gauge the accuracy of our approach and the effects of finite lattice size we have compared our results with those of Zwerger [6] for an infinite lattice (lines in Fig. 4); we show the latter for both finite and infinite nearest neighbor repulsions. We obtain very good agreement, particularly as we increase the number of adsorption sites. The small difference that does occur has our diffusivity lower at low coverage and higher around 1/2 ML.

However, this difference can be understood if we adapt the results of Zwerger for diffusion on an infinite lattice to that on a finite one, as outlined in Appendix C. The two diffusion coefficients will be denoted as $D^Z_{\text{inf}}, D^Z_{\text{fin}}$, respectively. In Figure 5, we compare these with that obtained from our eigenvalue spectrum, D_{eig}. One can see that D^Z_{fin} differs from D^Z_{inf}, more or less depending on the lattice size,

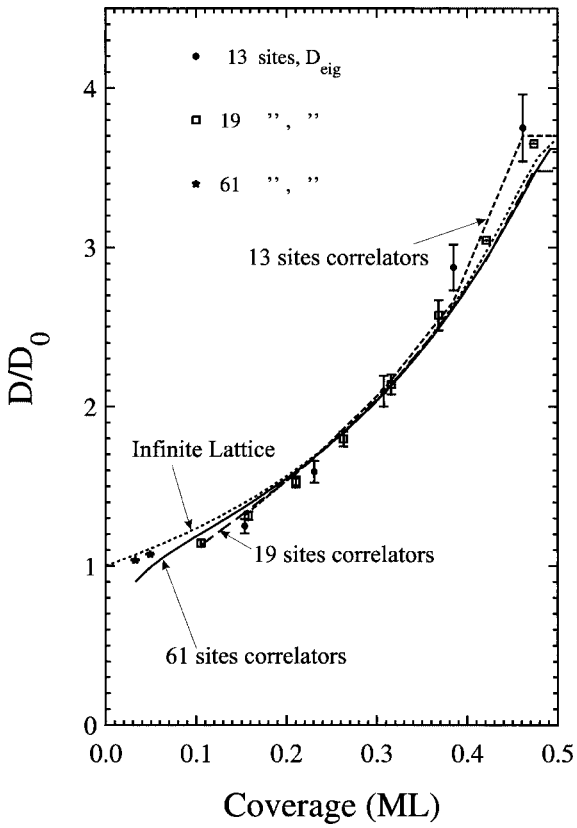

FIGURE 5. The diffusion coefficient as a function of coverage with nearest-neighbor repulsions ($\beta V_1 = 5$) and interaction kinetics. Symbols: diffusion coefficient, D_{eig}, derived from the eigenvalue spectrum for a finite lattice. Lines: diffusion coefficient given by Zwerger's result on an infinite lattice (D^Z_{inf}, dotted line) and as adapted to a finite lattice (D^Z_{fin}, dashed, long-dashed and solid). The lattice sizes used are 13, 19, and 61 sites.

but is in excellent agreement with $D_{\rm eig}$ for coverages above 1/4 ML; below 1/4 ML, both $D^Z_{\rm fin}$ and $D_{\rm eig}$ still agree very well.

4.2. ADSORBATE STRUCTURE

One might expect that all eigenvalues that do not correspond to the diffusive behavior of the system will have weights that vanish in the continuum limit, as occurs for the non-interacting case, [cf. (44)]. But it is clear from the eigenvalue spectrum in Figure 3 that, away from the low-q limit, there can be many eigenvalues with significant weight ($|C_\alpha(q)| > 0.02$). Provided these eigenvalues are small enough they, too, will contribute to the particle correlations, as well as the average occupation, in the long-time limit. In this repulsive case, these eigenvalues appear for larger values of q and their number increases with coverage. For 7/19 ML, they concentrate around $q = 8$. This corresponds to a wavelength of $\sim 2a$, which matches that of the ordered (equilibrium) structure expected for strong neighbor repulsions at 1/2 ML with alternate sites occupied:

○●○●○●○●○●○●○●○●○.

Here, because we cannot have 1/2 ML exactly, we also observe many, small eigenvalues at $q = 6, 7$ as well. We have confirmed, by examination of larger lattices, that we are not observing a finite-size effect. Indeed, the number of (relatively) significant eigenvalues increases with lattice size. As an example of this, we show the spectrum for only 3 particles on 61 sites, (Fig. 6). Compared with the similar coverage of 1/19 ML, for which all the weights must vanish except those of the diffusive eigenvalue, there are now many nondiffusive eigenvalues with significant weights.

Similarly, in the case of very strong attractive interactions ($\beta V = -5$) for 7/19 ML we have found that the dominant eigenvalues are around $q = 0$ and 1 with the former corresponding to the diffusive eigenvalue. The non-diffusive eigenvalue corresponds to a wavelength of $19a$ and the configuration expected for strong attraction between nearest neighbors:

●●●●●●●○○○○○○○○○○○○.

Such features are properly described by the long-time limit of the coherent structure factor:

$$S(q,t,t') = \frac{1}{N_s^2}\sum_{l,m}\langle n_l(t)n_m(t')\rangle e^{-2\pi i q(l+m)/N_s} - \tilde{n}_q(t)\tilde{n}_q(t'). \quad (50)$$

Although two-particle correlations are an output of our method and the structure factor would provide additional insight into the evolution of the system, as well as the diffusivity in the limit $q \to 0$, we have not attempted to construct S. It is not clear that we would see the same features in S as we have in our eigenvalue-weight spectra thus far. The selection of eigenvalues of large weight was done with one-particle averages in mind; it may be that for two-particle averages, eigenvalues of lower weight currently become important for their time evolution.

4.3. COMPLETE TIME EVOLUTION: TRANSIENTS

Finally, and to illustrate the information already available from the one-particle functions, we exhibit the full time evolution of an adsorbate towards equilibrium. In Figure 7 we show the evolution of the average occupation of selected sites on a lattice, as given by (36), for $N = 9, N_s = 17$, for strong particle repulsions ($\beta V_1 = 5$), interaction kinetics,

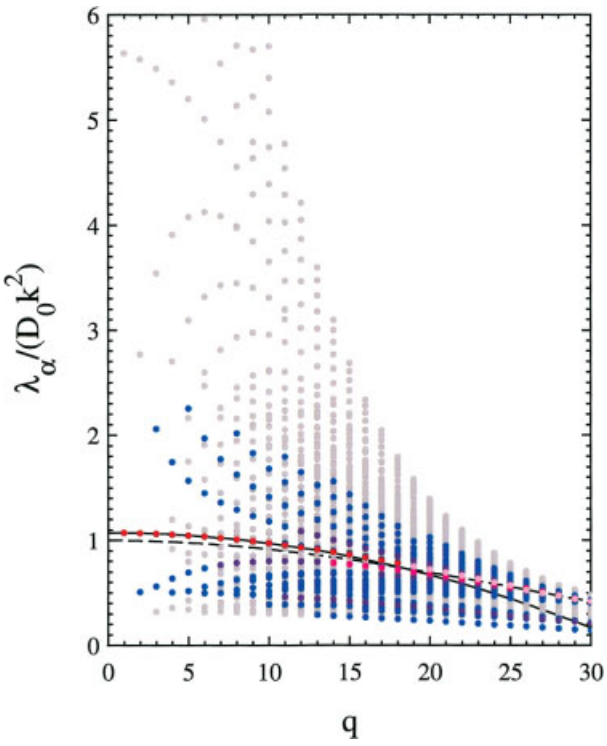

FIGURE 6. The eigenvalue spectrum at 3/61 ML on 61 sites with $\beta V_1 = 5$ and interaction kinetics. The color coding of the eigenvalue weights and description of the lines are as in Fig. 3.

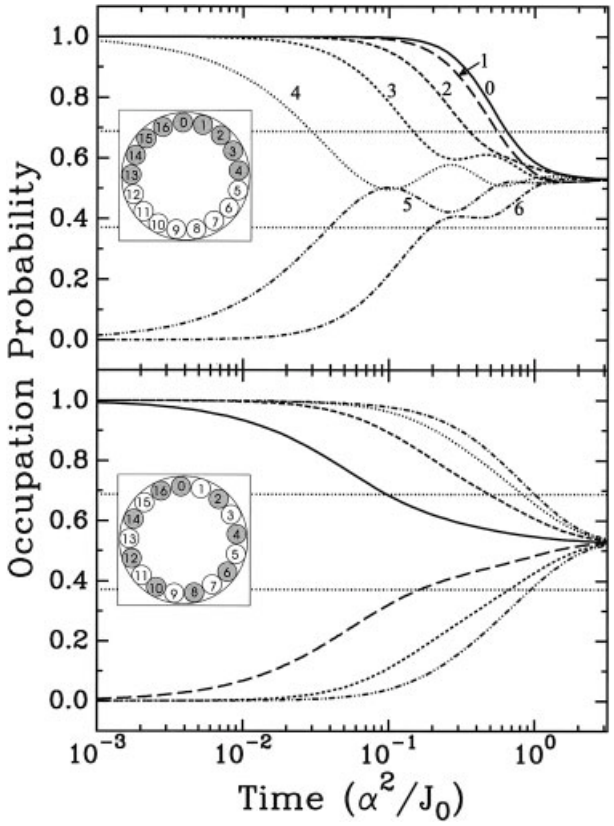

FIGURE 7. The time evolution of the average site occupations, $\langle n_l(t)\rangle$, of 9 particles on 17 sites with $\beta V_1 = 5$ and interaction kinetics for the two initial configurations shown. The sites being tracked are $l = 0$–6, indicated in the top panel. Horizontal lines are defined in the text. Time scale is logarithmic; $\alpha^2 = [N_s/(2\pi)]^2$.

and for two different initial conditions. We have scaled time by $\alpha^2 = [N_s/(2\pi)]^2$, so that the time to reach equilibrium is independent of the number of adsorption sites. The evolution of any particle correlation function has three different time scales: one for local equilibrium, a transient regime, and a diffusive regime. The first initial configuration (Fig. 7, upper panel) has all adsorbed particles on one "side" of the lattice. By symmetry, the time evolutions of sites $1 \rightarrow 6$ will be exactly those of sites $16 \rightarrow 11$. Let us follow the time evolution of site 4 in detail. The particle initially at this site is the first to move (other than that at site 13). The average occupation of any site reaches local equilibrium when the relative change of this occupation is less than, or of the order of, that of its root-mean-square fluctuation. The latter can be estimated by evaluating the equilibrium fluctuations for an infinite 1D lattice [9], $\sqrt{\langle \delta n_l^2 \rangle} = \sqrt{\partial\theta/\partial(\beta\mu)|_T}$. The range of this quantity about the coverage (9/17) is indicated by the two horizontal (dotted) lines in Figure 7. As can be seen, the occupation probability of site 4 approaches local equilibrium much faster than do sites 0–3. The transient regime for this quantity is reflected in the oscillatory behavior of site 4 occupation, thereafter, and mirrored in the evolution at site 5. This can be visualized as the particle moving to site 5, then back to site 4, then being "pushed" back to site 5 again by the particle at site 3. After sufficient time, such oscillations have decayed and the occupations of sites 0–8 have steadied, a gradient of population from site to site (not visible) occurs, and the adsorbate has entered the diffusive regime. The evolution is quite different with the initial configuration shown in Figure 7, (lower panel). As this would match the equilibrium configuration of a system with strong repulsion, but for the deletion of one particle and one site, some of the occupation probabilities now evolve on a slower time scale than in the upper panel. The particle at site 0 is the first to move, as it is the only one with a neighbor. This induces a ripple effect whereby the average occupation of site 1 adjusts upward (from zero), then that of site 2 downward, and so on, with even (odd)-numbered sites decreasing (increasing) in average occupation. Each site evolves on a different time scale, which increases with the separation from site 0.

5. Summary

A method is presented that transparently allows the solution of the master equation for the complete time evolution of various configurations of interacting particles on a finite 1D lattice, initially out of equilibrium. This was achieved by changing the representation of the configurations and restricting the lattice to a prime number of sites with periodic boundary conditions; a subsequent transform to reciprocal (q) space and the exploiting of symmetries of the system has reduced the problem to a consideration of computationally manageable sets of eigenvectors and eigenvalues of the transition rate matrix appearing in the master equation. The method also allows the extraction of the collective diffusion coefficient, directly, by considering eigenvalues with significant weight which survive in the evolution of the particle density in the hydrodynamic limit. In particular, as we increase the lattice size, we have excellent agreement with the coverage dependence for an infinite 1D lattice obtained from

linear response theory. The nondiffusive eigenvalues that also survive in the long-time limit, but for finite values of q, are associated with the ordered structures of the interacting particles.

In this investigation we have not considered some obvious extensions of our results. For example, the dependence of the diffusivity on the choice of hopping rates, as noted in the Introduction: One can alter the restriction on the rates as given in Eqs. (12) and (13). Indeed, if (13) is not satisfied, no analytic form of the diffusion coefficient exists within linear response theory; only approximate methods have been used so far [16]. In our approach, such alterations merely require a change of the form of the transition rate matrix. Similarly, the effects of multisite hops and adsorption–desorption processes can be tested easily within our framework. We note that there are a number of adsorption systems in which diffusion is predominantly in one dimension and in which investigations of the above effects are of interest [21]. Regardless, the extension of the method to two dimensions is desirable. This is straightforward, provided one retains the unique labeling of the shift representation. Thus, one places N particles on a torus of $N_s = N_1 \times N_2$ sites with N_1 and N_2 prime and N relatively prime to both N_1 and N_2. In this case, the number of primitives would still be given by Eq. (17). With corresponding shift numbers, $\mathbf{s} = (s_1, s_2)$, $\widetilde{s}_i = s_i/N_i$, to index the particle arrangements in orthogonal directions for a primitive, one would construct similar expressions; e.g., Eq. (23) becomes

$$\widetilde{P}(p, \mathbf{q}, t) = \frac{1}{N_s} \sum_{s_1=0}^{N_1-1} \sum_{s_2=0}^{N_2-1} e^{-2\pi i \mathbf{q}\cdot\widetilde{\mathbf{s}}} P(p, \mathbf{s}, t), \qquad (51)$$

with wavenumber $\mathbf{q} = (q_1, q_2)$.The entire formalism applies, only the computational complexity would change. Moreover, our approach of obtaining the diffusion coefficient from the resulting eigenvalues of the transition rate matrix has all the advantages associated with the 1D case, most importantly, the testing of dependence on adsorbate coverage and interactions.

ACKNOWLEDGMENTS

C. B. gratefully acknowledges financial support from the Killam Trust and the Alexander von Humboldt Foundation.

References

1. Ala-Nissila, T.; Ferrando, R.; Ying, S. C. Adv Phys 2002, 51, 949.
2. Haus, J. W.; Kehr, K. W. Phys Rep 1987, 150, 263.
3. Dieterich, W.; Fulde, P.; Peschel, I. Adv Phys 1980, 29, 527.
4. Allnatt, A. R.; Lidiard, A. Rep Prog Phys 1987, 50, 573.
5. Chudley, C. J.; Elliott, R. J. P Phys Soc Lond 1961, 77, 33.
6. Zwerger, W. Z Phys B 1981, 42, 333.
7. van Kampen, N. G. Stochastic Processes in Physics and Chemistry; North-Holland: New York, 1981.
8. van Kampen, N. G. Z Phys B: Condens Matter 1987, 68, 135.
9. Kreuzer, H. J. Nonequilibrium Thermodynamics and its Statistical Foundations; Oxford University Press: New York, 1981.
10. Kreuzer, H. J.; Payne, S. H. Computional Methods in Colloid and Interface Science; Marcel Dekker: New York, 1999.
11. Kreuzer, H. J.; Zhang, J. Appl Phys A, 1990, 51, 183.
12. Glauber, R. J. J Math Phys 1963, 4, 294.
13. Kreuzer, H. J. Langmuir 1992, 8, 774.
14. Kreuzer, H. J.; Gortel, Z. W. Physisorption Kinetics; Springer Series in Surface Sciences; Vol 1, Springer-Verlag: Berlin, 1986.
15. Payne, S. H.; Wierzbicki, A.; Kreuzer, H. J. Surf Sci 1993, 291, 242.
16. Singer, H.; Peschel, I. Z Phys B 1980, 39, 333.
17. Patchedjiev, S. Kinetic Lattice Gas Model for Adsorption, Desorption and Diffusion: An Investigation of Truncation Schemes; thesis; Dalhousie University: Halifax, Canada, 2002.
18. Stoer, J.; Bulirsch, R. Introduction to Numerical Analysis; 2nd ed.; Springer-Verlag: New York, 1992.
19. Kreuzer, H. J. In Diffusion at Interfaces: Microscopic Concepts; Vol 12; Grunze, M.; Kreuzer, H. J.; Weimer, J., Eds.; Springer-Verlag: Berlin, 1986; p 63.
20. Gaspard, P. Chaos, Scattering and Statistical Mechanics; Cambridge University Press: Cambridge, UK, 1998.
21. Linderoth, T. R.; Horch, S.; Laegsgaard, E.; Stensgaard, I.; Basenbacher, F. Phys Rev Lett 1997, 78, 4978.
22. Abramowitz, M.; Stegun, I. A. Handbook of Mathematical Functions; Dover: New York, 1972.

Appendix A

Within the choice of kinetics given by Eqs. (13) and (12) and nearest-neighbor interactions, one obtains the equation of motion for $\langle n_l \rangle$ by multiplying the master equation, (6), with n_l, summing over all microstates and making use of Eq. (14). After some cancellations, one obtains

$$\frac{d}{dt}\langle n_l\rangle(t) = J_0\{\langle n_{l-1}\rangle(t) - 2\langle n_l\rangle(t) + \langle n_{l+1}\rangle(t) + A_1[\langle n_{l-2}n_{l-1}(1-n_l)\rangle(t) + \langle(1-n_l)n_{l+1}n_{l+2}\rangle(t) - \langle n_{l-1}n_l(1-n_{l+1})\rangle(t) - \langle(1-n_l)n_{l+1}n_{l+2}\rangle(t)] + B_1[2\langle n_{l-1}(1-n_l)n_{l+1}\rangle(t) - \langle n_{l-2}(1-n_{l-1})n_l\rangle(t) - \langle n_l(1-n_{l+1})n_{l+2}\rangle(t)]\}. \quad \text{(A.1)}$$

Two- and three-site correlators appear with the coefficients A_1 and B_1; a coupling to four-site correlators occurs if the coefficient C_1 does not vanish. Equations of motion for these correlators can be generated similarly, which will contain yet higher-order correlations. In this manner, an infinite hierarchy of coupled equations is obtained. For examples of the hierarchy, but for a homogeneous system, see Ref. [15].

Appendix B

There exists a symmetry of our microstates that allows us to choose the eigenvalue weights in (37) to be real. Two particle arrangements that transform into each other when the contents of the sites l and $N_s - l(\mathrm{mod}N_s)$ are exchanged are, by definition, images of each other under the reflection operation R; we denote the mirror image of a primitive p by $R[p]$. It can be shown that R commutes with the matrices $\mathbf{S}$, $\mathbf{W}(q)$, hence $\mathbf{W}_s(q)$. Thus, as the eigenvalues of R are ± 1, the components of the eigenvectors $\mathbf{u}^s_\alpha(q)$ can be chosen to obey

$$u^s_\alpha(p,q) = \pm u^s_\alpha(R[p],q)^* \quad \text{(B.1)}$$

for $(+)$ symmetric and $(-)$ antisymmetric configurations. However, even if all eigenvalues of $\mathbf{W}(q)$ are distinct, one can still assign a unitary phase $e^{i\phi}$ to each eigenvector:

$$\mathbf{u}^s_\alpha(q) \to e^{i\phi}\mathbf{u}^s_\alpha(q). \quad \text{(B.2)}$$

These arbitrary phases show up in numerical diagonalization. If we choose to multiply all antisymmetric eigenvectors in Eq. B.1 by the phase factor $i = e^{i\pi/2}$, while leaving the symmetric subset unchanged, we have

$$u^s_\alpha(p,q) = u^s_\alpha(R[p],q)^*. \quad \text{(B.3)}$$

Similarly, $\widetilde{\Theta}(p,q)$, cf. Eq. (38), and $\widetilde{\Theta}(R[p],q)$ are complex conjugates of each other. In the summation over primitives to form $C_\alpha(q)$, each primitive and its mirror image appear, the respective terms in the summand are complex conjugate (but real for palindromic primitives, obeying $p = R[p]$) so that $C_\alpha(q)$ must be real.

Under a second symmetry operation imposed by our choice of kinetics, i.e., particle-hole exchange, the sign of $C_\alpha(q \neq 0)$ changes. If we denote the site-matching Kronecker delta for N particles on N_s sites, appearing in (22), by $\Theta^+ = \Theta([p|s], n_l)$ then, under particle-hole exchange, this converts to $\Theta^- = \Theta([p'|s], 1-n_l)$, where p' is a primitive for $N_s - N$ particles on N_s sites. We have $\Theta^+ + \Theta^- = 1$; the Fourier transform of this relation, cf. (38), yields $\widetilde{\Theta}^+ + \widetilde{\Theta}^- = \delta_{q,0}$. Thus, $\widetilde{\mathbf{\Theta}}(q \neq 0)$ changes sign with particle-hole exchange. However, the transition rate matrix $\mathbf{W}(q)$ is invariant, hence also its eigenvectors $\mathbf{u}_\alpha(q), \mathbf{v}_\alpha(q)$. Thus, $C_\alpha(q \neq 0)$ must change sign.

Appendix C

In this Appendix, we adapt Zwerger's [6] result for the diffusion coefficient on an infinite 1D lattice to that on a finite one. Using linear response theory, Zwerger expressed the coefficient in terms of the isothermal susceptibility and particle correlators. For the case of interaction kinetics, cf. (12) and particle-hole symmetry, his result can be written as

$$\frac{D}{D_0} = \left.\frac{\partial\beta\mu}{\partial\theta}\right|_T [(\theta - \langle\bullet\bullet\rangle) + A_1(\langle\bullet\bullet\rangle - \langle\bullet\times\bullet\rangle)], \quad \text{(C.1)}$$

where the derivative of the chemical potential, μ, with respect to coverage is given by

$$\left.\frac{\partial\beta\mu}{\partial\theta}\right|_T = \frac{1}{\alpha\theta(1-\theta)} \quad \text{(C.2)}$$

with

$$\alpha = \sqrt{1 - 4\theta(1-\theta)(1-y)} \quad \text{(C.3)}$$

and

$$A_1 = \frac{1-y}{1+y}. \quad \text{(C.4)}$$

Here $y = e^{-\beta V_1}$. The two-particle (equilibrium) correlators $\langle\bullet\bullet\rangle$, $\langle\bullet\times\bullet\rangle$, are analytic functions of coverage [15],

$$\langle\bullet\bullet\rangle = \theta\left(1 - 2\frac{1-\theta}{1+\alpha}\right) \quad \text{(C.5)}$$

$$\langle\bullet\times\bullet\rangle = \langle\bullet\bullet\bullet\rangle + \langle\bullet\circ\bullet\rangle = \frac{\langle\bullet\bullet\rangle^2}{\langle\bullet\rangle} + \frac{\langle\bullet\circ\rangle^2}{\langle\circ\rangle}. \quad \text{(C.6)}$$

We have used the notation $\langle\bullet\rangle = \langle n_l\rangle$, $\langle\circ\rangle = \langle 1 - n_l\rangle = 1 - \langle\bullet\rangle$, $\langle\bullet\circ\rangle = \langle\bullet\rangle - \langle\bullet\bullet\rangle$, etc. The factorizations of the 3-site correlators into products of 2-site ones, exhibited in Eq. (C.6) are only exact for an infinite lattice.

We have adapted Eq. (C.1) to a finite lattice as follows. Since there can only be an integer number of particles on a finite lattice, we replace the derivative of the chemical potential above with finite differences of the free energy yielding

$$\left.\frac{\partial\beta\mu}{\partial\theta}\right|_T \to -N_s\{\ln[Z(N+1,N_s,T) \times Z(N-1,N_s,T)/Z^2(N,N_s,T)]\}. \quad \text{(C.7)}$$

The lattice partition function for N particles on N_s sites can be expressed in terms of hypergeometric functions [22]:

$$Z(N,N_s,T) = A_1\,{}_2F_1\big(1-N,1-N_s+N,2;y^{-1}\big). \quad \text{(C.8)}$$

All correlators on a finite lattice can be represented this way as well. The relevant ones are

$$\langle\bullet\circ\rangle = \frac{1}{N_s}\frac{{}_2F_1(1-N,1-N_s+N,1;y^{-1})}{{}_2F_1(1-N,1-N_s+N,2;y^{-1})}$$

$$\langle\bullet\circ\circ\rangle = \frac{1}{N_s}\frac{{}_2F_1(1-N,2-N_s+N,1;y^{-1})}{{}_2F_1(1-N,1-N_s+N,2;y^{-1})}$$

$$\langle\bullet\bullet\bullet\rangle = \frac{N-2}{N_s}\frac{{}_2F_1(3-N,1+N-N_s,2;y^{-1})}{{}_2F_1(1-N,1+N-N_s,2;y^{-1})}, \quad \text{(C.9)}$$

with $\langle\bullet\times\bullet\rangle = \langle\bullet\circ\rangle - \langle\bullet\circ\circ\rangle + \langle\bullet\bullet\bullet\rangle$, since $\langle\bullet\circ\rangle = \langle\bullet\circ\bullet\rangle + \langle\bullet\circ\circ\rangle$ by conservation of probability.